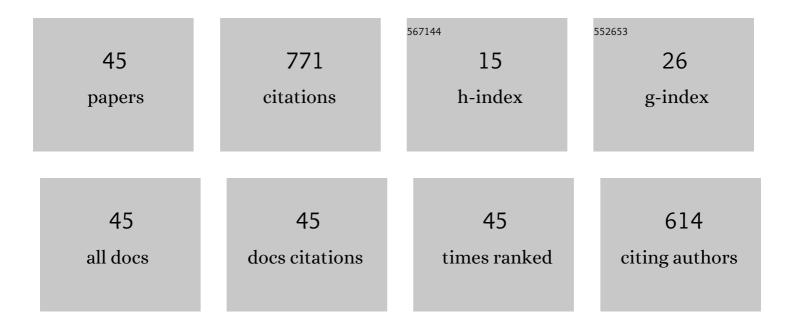
Zhidan Sun

List of Publications by Year in descending order

Source: https://exaly.com/author-pdf/7064111/publications.pdf Version: 2024-02-01



ΖΗΙΔΑΝ SUN

#	Article	IF	CITATIONS
1	Optimization of shot peening parameters for AA7B50-T7751 using response surface methodology. Simulation Modelling Practice and Theory, 2022, 115, 102426.	2.2	6
2	Estimation of fatigue crack initiation in the very high cycle fatigue regime for AA7075-T6 alloy using crystal plasticity finite element method. Journal of Materials Science, 2022, 57, 10649-10663.	1.7	4
3	Experimental study of a CoCrMo alloy treated by SMAT under rotating bending fatigue. Procedia Structural Integrity, 2022, 38, 283-291.	0.3	3
4	Investigation of the Fatigue Life Scatter for AA7075-T6 Using Crystal Plasticity Finite Element Method in the High to Very High Cycle Fatigue Regime. Integrating Materials and Manufacturing Innovation, 2022, 11, 198-213.	1.2	2
5	Numerical characterization of shot peening induced work hardening gradient and verification based on FEM analysis. International Journal of Solids and Structures, 2022, 244-245, 111586.	1.3	6
6	Literature Review on the Fatigue Properties of Materials Processed by Surface Mechanical Attrition Treatment (SMAT). Metals, 2022, 12, 775.	1.0	5
7	Effect of Surface Mechanical Attrition Treatment on Torsional Fatigue Properties of a 7075 Aluminum Alloy. Metals, 2022, 12, 785.	1.0	6
8	Effect of transformed β phase on fish-eye ductile crack initiation of a Ti-6Al-4V alloy in very high cycle fatigue regime. Materials Letters, 2021, 287, 129283.	1.3	7
9	Elastic and elastic-plastic stress release due to material removal in measurement of in-depth residual stresses. International Journal of Pressure Vessels and Piping, 2021, 191, 104380.	1.2	8
10	Micromechanisms of crack initiation of a Ti-8Al-1Mo-1V alloy in the very high cycle fatigue regime. International Journal of Fatigue, 2021, 150, 106314.	2.8	10
11	Influence of surface coverage on the fatigue behavior of a shot peened AA7B50-T7751 alloy. Surface Topography: Metrology and Properties, 2021, 9, 035041.	0.9	1
12	In-situ EBSD investigation of thermal stability of a 316L stainless steel nanocrystallized by Surface Mechanical Attrition Treatment. Materials Letters, 2020, 263, 127249.	1.3	6
13	Effect of Turning on the Surface Integrity and Fatigue Life of a TC11 Alloy in Very High Cycle Fatigue Regime. Metals, 2020, 10, 1507.	1.0	6
14	Effect of surface mechanical attrition treatment on high cycle and very high cycle fatigue of a 7075-T6 aluminium alloy. International Journal of Fatigue, 2020, 139, 105798.	2.8	30
15	Investigation of crack initiation mechanism of a precipitation hardened TC11 titanium alloy under very high cycle fatigue loading. Materials Science & Engineering A: Structural Materials: Properties, Microstructure and Processing, 2020, 776, 138989.	2.6	20
16	Characterization of gradient properties generated by SMAT for a biomedical grade 316L stainless steel. Materials Characterization, 2019, 155, 109788.	1.9	21
17	Investigation of ductile damage during surface mechanical attrition treatment for TWIP steels using a dislocation density based viscoplasticity and damage models. Mechanics of Materials, 2019, 129, 279-289.	1.7	20
18	Fatigue properties and cracking mechanisms of a 7075 aluminum alloy under axial and torsional loadings. Procedia Structural Integrity, 2019, 19, 637-644.	0.3	8

Zhidan Sun

#	Article	IF	CITATIONS
19	Experimental analysis and constitutive modelling of cyclic behaviour of 316L steels including hardening/softening and strain range memory effect in LCF regime. International Journal of Plasticity, 2018, 107, 54-78.	4.1	92
20	Reconstruction of residual stress and work hardening and their effects on the mechanical behaviour of a shot peened structure. Mechanics of Materials, 2018, 127, 100-111.	1.7	24
21	Low cycle fatigue of 316L stainless steel processed by surface mechanical attrition treatment (SMAT). MATEC Web of Conferences, 2018, 165, 15002.	0.1	2
22	Very High Cycle Fatigue of a Cast Aluminum Alloy: Size Effect and Crack Initiation. Journal of Materials Engineering and Performance, 2018, 27, 5406-5416.	1.2	18
23	Fatigue crack initiation and propagation of 100Cr6 steel under torsional loading in very high cycle regime. MATEC Web of Conferences, 2018, 165, 20003.	0.1	2
24	Comparative study of the effects of surface mechanical attrition treatment and conventional shot peening on low cycle fatigue of a 316L stainless steel. Surface and Coatings Technology, 2018, 349, 556-566.	2.2	60
25	Constitutive modeling of TWIP/TRIP steels and numerical simulation of single impact during Surface Mechanical Attrition Treatment. Mechanics of Materials, 2018, 122, 69-75.	1.7	12
26	Effect of Surface Mechanical Attrition Treatment on the very high cycle fatigue behavior of TC11. MATEC Web of Conferences, 2018, 165, 09001.	0.1	5
27	Effect of surface mechanical attrition treatment on low cycle fatigue properties of an austenitic stainless steel. International Journal of Fatigue, 2017, 103, 309-317.	2.8	61
28	Experimental study of microstructure changes due to low cycle fatigue of a steel nanocrystallised by Surface Mechanical Attrition Treatment (SMAT). Materials Characterization, 2017, 124, 117-121.	1.9	42
29	Numerical simulation of mechanical deformation of semi-solid material using a level-set based finite element method. Modelling and Simulation in Materials Science and Engineering, 2017, 25, 065020.	0.8	5
30	Lifetime prediction of a viscoplastic lead-free solder in power electronics modules under passive temperature cycling. Mechanics and Industry, 2016, 17, 306.	0.5	2
31	Numerical modeling and simulation of intergranular fracture due to dynamic embrittlement for a CuNiSi alloy. Mechanics Research Communications, 2016, 75, 81-88.	1.0	4
32	Continuum Damage Approach for Fatigue Life Prediction of Viscoplastic Solder Joints. Journal of Mechanics, 2015, 31, 525-531.	0.7	9
33	Analytical homogenization modeling and computational simulation of intergranular fracture in polycrystals. International Journal of Fracture, 2015, 193, 59-75.	1.1	8
34	Numerical study of anisotropic failure in wood under large deformation. Materials and Structures/Materiaux Et Constructions, 2015, 48, 1977-1993.	1.3	6
35	Micro-pillar compression tests to characterize the mechanical behavior of a nanocrystalline layer induced by SMAT in a 316L stainless steel. Materiaux Et Techniques, 2015, 103, 304.	0.3	6
36	Fatigue properties of a biomedical 316L steel processed by surface mechanical attrition. IOP Conference Series: Materials Science and Engineering, 2014, 63, 012021.	0.3	8

ZHIDAN SUN

#	Article	IF	CITATIONS
37	Homogenization scheme for brittle intergranular decohesion in polycrystalline aggregates. Mechanics Research Communications, 2014, 55, 114-119.	1.0	5
38	Effects of voids on thermal-mechanical reliability of lead-free solder joints. MATEC Web of Conferences, 2014, 12, 04026.	0.1	6
39	Fatigue Crack Growth under High Pressure of Gaseous Hydrogen in a 15-5PH Martensitic Stainless Steel: Influence of Pressure and Loading Frequency. Metallurgical and Materials Transactions A: Physical Metallurgy and Materials Science, 2013, 44, 1320-1330.	1.1	35
40	Prediction of thermo-mechanical fatigue for solder joints in power electronics modules under passive temperature cycling. Engineering Fracture Mechanics, 2013, 107, 48-60.	2.0	16
41	A thermo-mechanical cohesive zone model for solder joint lifetime prediction. International Journal of Fatigue, 2013, 49, 18-30.	2.8	44
42	Fatigue crack propagation under gaseous hydrogen in a precipitation-hardened martensitic stainless steel. International Journal of Hydrogen Energy, 2011, 36, 8641-8644.	3.8	40
43	Dynamic embrittlement during fatigue of a Cu–Ni–Si alloy. Materials Science & Engineering A: Structural Materials: Properties, Microstructure and Processing, 2011, 528, 6334-6337.	2.6	13
44	3D finite element model of semi-solid permeability in an equiaxed granular structure. Computational Materials Science, 2010, 49, 158-170.	1.4	31
45	Dynamic embrittlement at intermediate temperature in a Cu–Ni–Si alloy. Materials Science & Engineering A: Structural Materials: Properties, Microstructure and Processing, 2008, 477, 145-152.	2.6	46